JOURNAL OF GEOPHYSICAL RESEARCH, VOL. 104, NO. D19, PAGES 23,697–23,707, OCTOBER 20, 1999

Effects of aerosols on tropospheric photolysis rates in clear and cloudy atmospheres

Hong Liao

Division of Engineering and Applied Science, California Institute of Technology, Pasadena

Yuk L. Yung

Division of Geological and Planetary Sciences, California Institute of Technology, Pasadena

John H. Seinfeld

Division of Engineering and Applied Science, California Institute of Technology, Pasadena

Abstract. The effect of aerosols on 14 tropospheric photolysis reactions is examined under noncloudy and cloudy sky conditions by using a detailed one-dimensional radiative transfer model. Pure $(NH_4)_2SO_4$, pure soot, and internal and external mixtures of the two aerosols, as well as mineral dust aerosol, are considered. Nonabsorbing aerosol generally enhances photolysis rates above and in the upper part of the aerosol layer in both noncloudy and cloudy atmospheres, with the enhancement effect reduced in the presence of clouds. In contrast, soot aerosol reduces photolysis rates under both noncloudy and cloudy sky conditions, with the reduction accentuated by a cloud layer. Mixtures of absorbing and nonabsorbing aerosols may produce enhancement or reduction in photolysis rates under clear sky conditions, whereas they generally reduce rates when a cloud is present. In the absence of cloud, sulfate aerosol at urban levels enhances tropospheric average photolysis rates from 11 to 18% for the 14 reactions studied; soot aerosol decreases tropospheric average rates from 6 to 11%. In the presence of a 500-m-thick stratus cloud, sulfate aerosol enhances each of 14 tropospheric average photolysis rates by about 5%; soot aerosol decreases tropospheric average photolysis rates from 9 to 19%.

1. Introduction

Solar radiation drives the chemistry of the troposphere through the photodissociation of a number of molecules. The local photolysis rate of an atmospheric species i, $J(i)$ (s^{-1}), is given by

$$J(i) = \int_{\lambda_1}^{\lambda_2} \sigma_i(\lambda,T)\phi_i(\lambda,T)F(\lambda)d\lambda, \qquad (1)$$

where $\sigma_i(\lambda,T)$ (cm^2) is the wavelength and temperature-dependent absorption cross section of species i, $\phi_i(\lambda,T)$ is the quantum yield, and $F(\lambda)$ (photons cm^{-2} nm^{-1} s^{-1}) is the solar actinic flux. In the troposphere, the wavelength range of interest is approximately $\lambda_1 = 290$ nm to $\lambda_2 = 700$ nm.

Calculation of photolysis rates requires accurate specification of actinic flux, which in the troposphere depends on solar zenith angle, surface albedo, molecular absorption, Rayleigh scattering, and the presence of clouds and aerosols. The effects of molecular absorption and Rayleigh scattering on actinic flux are relatively well known and are routinely modeled. Among all the absorbing gases, ozone has the most significant effect on tropospheric chemistry by altering photolysis rates [*Liu and Trainer*, 1988; *Thompson et al.*, 1989; *Madronich and Granier*, 1992; *Fuglestvedt et al.*, 1994; *Ma*, 1995]. As shown by *Fuglestvedt et al.* [1994], for the period 1970-1990, stratospheric ozone depletion led to a reduction of 4.5% in global annually averaged total O_3, which increased the global annual average surface photodissociation rate of O_3 to $O(^1D)$ by 6.3%.

Radiative transfer in a cloudy atmosphere and its relation to photochemistry have been studied quite extensively [*Thompson*, 1984; *Madronich*, 1987a,b; *Tsay and Stamnes*, 1992; *van Weele and Duynkerke*, 1993; *Krol and van Weele*, 1997; *Matthijsen et al.*, 1997, 1998; *Crawford et al.*, 1999]. In comparison to clear sky, an optically thick cloud is predicted to increase photolysis rates in the upper part of the cloud and above cloud, while reducing those below cloud.

Aerosols scatter and absorb UV radiation and consequently either enhance or reduce actinic flux and/or photolysis rates. Studies of the effects of aerosols on UV radiation have been carried out by *Liu et al.* [1991], *Forster* [1995], *Reuder et al.* [1996], *Ma and Guicherit* [1997], *Erlick and Frederick* [1998], *Erlick et al.* [1998], *Papayannis et al.* [1998], *Repapis et al.* [1998], *Jacobson* [1999], and *Reuder and Schwander* [1999]. Ma and Guicherit studied the effects of air pollutants on surface UV-B radiation by using a multilayer radiative transfer model and found that the increase of tropospheric pollution in nonurban regions over that last

Paper number 1999JD900409.
0148-0227/99/1999JD900409$09.00

50-100 years has reduced the surface UV-B, offsetting the effect of the increase due to stratospheric ozone depletion. Recently, Reuder and Schwander showed that potential day-to-day variability in nonurban atmospheric aerosols produces changes of spectrally integrated actinic flux by 10-50%. Jacobson demonstrated that nitrated and aromatic aerosols may be important in reducing UV radiation. Measurements in Athens, Greece, showed that urban aerosols can reduce clear sky UV-B radiation by as much as 40% [*Papayannis et al.*, 1998; *Repapis et al.*, 1998]. Studies of the effects of tropospheric aerosols on photolysis rates have been carried out by *Demerjian et al.* [1980], *Ruggaber et al.* [1994], *Lantz et al.* [1996], *Castro et al.* [1997], *Dickerson et al.* [1997], *Landgraf and Crutzen* [1998], and *Jacobson* [1998]. Scattering aerosols in the boundary layer accelerate photochemical reactions within and above the aerosol layer [*Ruggaber et al.*, 1994; *Dickerson et al.*, 1997; *Landgraf and Crutzen*, 1998; *Jacobson*, 1998], while absorbing aerosols decrease photolysis rates [*Ruggaber et al.*, 1994; *Dickerson et al.*, 1997; *Jacobson*, 1998]. Effects of aerosols on photolysis rates are sensitive to the aerosol optical depth, single-scattering albedo, and vertical profile, as well as relative humidity and solar zenith angle [*Ruggaber et al.*, 1994].

Even though cloud and aerosol effects have been well studied separately, aerosol effects on photolysis rates in the presence of clouds have not yet been studied systematically. The goal of this work is to evaluate the impact of aerosols on tropospheric photolysis rates, with emphasis on the interaction between cloud and aerosol layers. This interaction is important because stratus clouds, those that are primarily responsible for the reflection of UV and visible radiation, frequently occur near the Earth's surface. Since scattering by aerosols below a low-level stratus cloud can be shielded by the cloud and aerosol absorption above the cloud can be significantly enhanced by the presence of the cloud [*Liao and Seinfeld*, 1998], we expect, as is shown in this study, that the effects of aerosols on photolysis rates in the presence of clouds can be quite different from those under clear sky conditions.

To explore the qualitative effect of aerosol optical properties and to span the range from nonabsorbing to strongly absorbing particles, $(NH_4)_2SO_4$ and soot aerosols are taken as representative of these extremes of tropospheric aerosols, in both internal and external mixtures. We consider also the effect of mineral dust aerosol on photolysis rates.

2. Radiative Transfer Model

We calculate actinic flux with the one-dimensional discrete ordinate radiative transfer (DISORT) model [*Stamnes et al.*, 1988]. DISORT uses the discrete ordinate method [*Chandrasekhar*, 1960] to solve the radiative transfer equation, and it uses the δ-M method [*Wiscombe*, 1977] to compute fluxes efficiently in scattering media with strongly asymmetric phase functions. The accuracy of DISORT has been confirmed under both clear and cloudy sky conditions. By comparing $J(NO_2)$ calculated with DISORT with that measured in the summer of 1995 at Greenbelt, Maryland, *Dickerson et al.* [1997] showed that clear sky predictions and measurements of $J(NO_2)$ agreed over a broad range of optical depths and zenith angles. It was shown by *Matthijsen et al.* [1998] that in the presence of clouds, modeled UV irradiances were close to the measured values; the difference was found to be within approximately 5 W m^{-2}.

The vertical resolution, spectral resolution, and number of streams of the code can be selected freely. In this study, we use 80 vertical layers from 0 to 70 km, with a vertical resolution of 100 m in the lowest 3 km, 200 m between 3 and 4 km, 1 km between 4 and 50 km, and 5 km between 50 and 70 km. Pressure, temperature, ozone, and number density of air are from the U.S. Standard Atmosphere (1976). Actinic flux calculations are performed in the wavelength region of 290 – 700 nm, with spectral intervals of 1 nm between 290 and 330 nm, 2 nm between 330 and 600 nm, and 5 nm between 600 and 700 nm. The highest resolution is taken at the shortest wavelengths where ozone absorption changes rapidly and where most photodissociation reactions of interest occur. The number of streams is set equal to 16.

The temperature-dependent ozone absorption cross section data are those reported by *Malicet et al.* [1995] (290 – 345 nm) at 218 K, 228 K, 243 K, 273 K, and 295 K, and by *World Meteorological Organization* (*WMO*) [1985] (345 – 700 nm) at 203 K and 273 K. Solar irradiance data are taken from *Woods et al.* [1996] for wavelengths ≤ 410.5 nm with a wavelength resolution of 1 nm and from *Neckel and Labs* [1984] for wavelengths > 410.5 nm with a resolution of 1 nm (wavelengths ≤ 630 nm) and 2 nm (wavelengths > 630 nm), respectively. The spectral surface albedo follows that of *Demerjian et al.* [1980] for land surface: 290 – 400 nm (0.05), 400 – 450 nm (0.06), 450 – 500 nm (0.08), 500 – 550 nm (0.10), 550 – 600 nm (0.11), 600 – 640 nm (0.12), 640 – 660 nm (0.135), and 660 – 700 nm (0.15).

3. Aerosol and Cloud Specification

When $(NH_4)_2SO_4$, soot, and mixtures thereof are present, we assume that an aerosol layer extends from the Earth's surface to 5 km, with the mass concentration of each species decreasing linearly from its value at the surface to 0.1 of its surface value at 3-km altitude and remaining constant from 3 to 5 km. Column burdens of 12.5 mg m^{-2} for $(NH_4)_2SO_4$ and 2.5 mg m^{-2} for soot are representative of continental conditions [*Liao and Seinfeld*, 1998]. For urban conditions, column burdens of 125 mg m^{-2} for $(NH_4)_2SO_4$ and 25 mg m^{-2} for soot are assumed. Whereas an $(NH_4)_2SO_4$ column burden of 125 mg m^{-2} is somewhat high for sulfate alone, this value can account for the presence of other essentially nonabsorbing components, such as nitrate. When mineral dust aerosol is considered, a uniform layer with a column burden of 100 mg m^{-2} is assumed at 3- to 6- km altitude. On the basis of the analysis of *Dentener et al.* [1996], 100 mg m^{-2} is roughly the annual average column dust burden over North Africa and Asia.

Aerosol optical properties are calculated with the code ELSIE [*Sloane*, 1984, 1986; *Sloane and Wolff*, 1985; *Sloane et al.*, 1991]. The dry mass size distributions of $(NH_4)_2SO_4$, soot, and mineral dust particles are assumed to be lognormal, with mean diameter of 0.5 μm and geometric standard deviation of 2.0 for $(NH_4)_2SO_4$, 0.1 μm and 2.0 for soot, and 2.0 μm and 2.0 for mineral dust particles, respectively. Refractive indices for $(NH_4)_2SO_4$, soot, and water are from *Toon et al.* [1976], *World Climate Program* [1986] and *Hale and Querry* [1973], respectively. The refractive index of dust from the world's desert regions varies significantly [*Patterson et al.*,

1977; *Sokolik et al.*, 1993]. For the mineral dust refractive index, we assume a real part of 1.50 and use curve 8 in Figure 1 of *Sokolik et al.* [1993] as the imaginary part, k, in the wavelength region of 290 to 700 nm. (Thus $k = 0.006$ at 500 nm.) Densities are taken to be 1.76 g cm^{-3} for $(NH_4)_2SO_4$, 1.70 g cm^{-3} for soot, and 2.5 g cm^{-3} for mineral dust. In the lowest 5 km of the U.S. Standard Atmosphere, a uniform relative humidity of 50% is a reasonable approximation and is used to calculate the hygroscopic and optical properties of the aerosol. Liquid water mass associated with pure $(NH_4)_2SO_4$ particles and mixed $(NH_4)_2SO_4$-soot particles is calculated by using gas-aerosol thermodynamic theory [*Pilinis and Seinfeld*, 1987; *Kim et al.*, 1993a,b]. It is assumed that soot and mineral dust are nonhygroscopic.

Particle index of refraction is calculated as a volume-weighted average of the indices of refraction of its components. For an external mixture of $(NH_4)_2SO_4$ (denoted s) and soot (denoted c), the single scattering albedo ω and asymmetry factor g are calculated by [*d'Almeida et al.*, 1991]

$$\omega = \frac{\omega_s\sigma_s + \omega_c\sigma_c}{\sigma_s + \sigma_c}, \tag{2}$$

$$g = \frac{g_s\omega_s\sigma_s + g_c\omega_c\sigma_c}{\omega_s\sigma_s + \omega_c\sigma_c}, \tag{3}$$

where σ_s and σ_c are the total extinction cross sections of sulfate and carbon particles, respectively.

When a cloud is present, we assume a stratus cloud layer centered at 950-m altitude with a thickness that can vary from 100 to 1000 m. Nominal cloud thickness is taken to be 500 m. Liquid water content, lwc, within the cloud is assumed to increase linearly with increasing height with a vertically averaged value of 0.2 g m^{-3}. An effective cloud droplet radius r_e of 10 μm is assumed, and the cloud optical depth over a layer of thickness dz is estimated by [*Slingo and Schrecker*, 1982]

$$\tau_{cloud} \approx \frac{3}{2}\frac{\text{lwc} \times dz}{\rho_w r_e}, \tag{4}$$

where ρ_w is the density of water. The asymmetry factor of the cloud layer is assumed to be 0.85 [*Matthijsen et al.*, 1998]. Aerosol particles are assumed to be present interstitially within the cloud. Since hygroscopic sulfate particles are expected to be scavenged by cloud droplets, this assumption leads to a small overestimation of photolysis rates above clouds and a slight underestimation of those within and below clouds.

A summary of total optical depth of the major atmospheric components considered in this study is given in Table 1. Vertical profiles of optical depth are shown in Figure 1 for Rayleigh scattering, ozone absorption, and urban sulfate aerosol. The optical depth is defined as that of a layer of 1-km thickness. The optical depth of Rayleigh scattering and aerosols is larger at UV wavelengths than it is at visible wavelengths; that of mineral dust is more or less constant over these wavelengths (Table 1).

Photolysis rates are computed by equation (1). Sources of absorption cross section and quantum yield data are listed in Table 2 for 14 photolysis reactions of importance in tropospheric chemistry.

Table 1. Total Optical Depth for Major Atmospheric Components Considered in This Study

Atmospheric Components	Total Optical Depth λ= 300 nm	Total Optical Depth λ= 400 nm
Rayleigh molecules	1.22	0.36
Ozone	3.34	0.00
Aerosols		
Pure $(NH_4)_2SO_4$ (continental)	0.13	0.09
Pure $(NH_4)_2SO_4$ (urban)	1.34	0.92
Pure soot (continental)	0.03	0.02
Pure soot (urban)	0.26	0.18
Internal mixture (urban)	1.63	1.12
External mixture (urban)	1.60	1.10
Mineral dust	0.11	0.12
Cloud (500 m thick)	15.0	15.0

4. Effects of Aerosols on Tropospheric Photolysis Rates

We have performed detailed calculations of photolysis as a function of altitude, aerosol, and cloud state for all 14

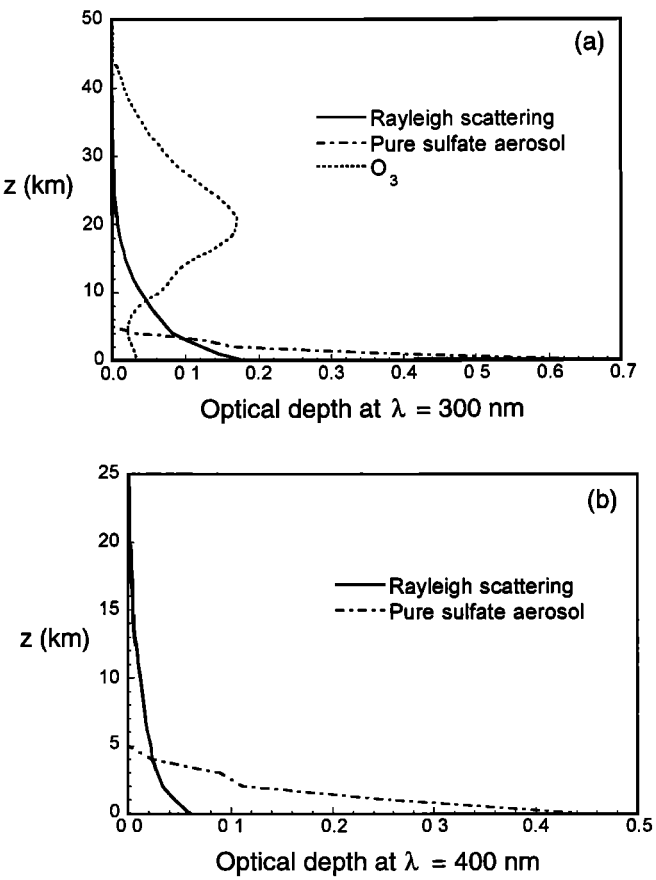

Figure 1. Profiles of optical depth per km for Rayleigh scattering, ozone absorption, and urban sulfate scattering at λ= 300 nm (a) and 400 nm (b). Profiles are obtained by dividing the atmosphere into layers of 1 km.

Table 2. Absorption Cross Section and Quantum Yield Data Used in Present Work

Photolysis Reactions	Absorption Cross Section	Quantum Yield (ϕ)	Wavelength Range, nm
$O_3 \rightarrow O(^3P) + O_2$	*Malicet et al.* [1995] *WMO* [1985]	*DeMore et al.* [1997]	290 – 700
$O_3 \rightarrow O(^1D) + O_2$	*Malicet et al.* [1995]	*DeMore et al.* [1997][a] *Takahashi et al.* [1998]	290 – 329
$NO_2 \rightarrow NO + O$	*DeMore et al.* [1997]	*DeMore et al.* [1997]	290 – 424
$NO_3 \rightarrow NO + O_2$	*Sander* [1986]	*Johnston et al.* [1996]	400 – 691
$NO_3 \rightarrow NO_2 + O$	*Sander* [1986]	*Johnston et al.* [1996]	400 – 691
$N_2O_5 \rightarrow NO_3 + NO_2$	*DeMore et al.* [1997]	$\phi = 1.0$	290 – 380
$H_2O_2 \rightarrow OH + OH$	*DeMore et al.* [1997]	$\phi = 1.0$	290 – 350
$HONO \rightarrow OH + NO$	*DeMore et al.* [1997]	$\phi = 1.0$	310 – 396
$HO_2NO_2 \rightarrow HO_2 + NO_2$	*DeMore et al.* [1997]	$\phi = 0.67$	290 – 325
$HO_2NO_2 \rightarrow OH + NO_3$	*DeMore et al.* [1997]	$\phi = 0.33$	290 – 325
$HCHO \rightarrow HCO + H$	*DeMore et al.* [1997]	*DeMore et al.* [1997]	301 – 356
$HCHO \rightarrow CO + H_2$	*DeMore et al.* [1997]	*DeMore et al.* [1997]	301 – 356
$CH_3OOH \rightarrow CH_3O + OH$	*DeMore et al.* [1997]	$\phi = 1.0$	290 – 360
$CH_3COCH_3 \rightarrow$ products	*Gierczak et al.* [1998]	*Gierczak et al.* [1998]	290 – 349

[a] The values of $\phi(O(^1D))$ recommended by *DeMore et al.* [1997] do not include the generation of $O(^1D)$ from spin-forbidden channel $O_3 + h\nu \rightarrow O(^1D) + O_2(a^1\Delta_g)$. For this channel a temperature-independent quantum yield of 0.08 in the wavelength range 318 - 329 nm has been determined by *Takahashi et al.* [1998] and is included in the present calculation.

photochemical reactions in Table 2; in the interest of space, we present here only $J(O_3 \rightarrow O(^1D))$, $J(NO_2)$, and $J(HCHO)$. Tropospherically averaged photolysis rates are given in section 4.1 for all 14 reactions.

4.1. Effect of Sulfate Aerosol on Photolysis Rates

The impact of sulfate aerosol on $J(O_3 \rightarrow O(^1D))$, $J(NO_2)$, and $J(HCHO)$ at 0° solar zenith angle is shown in Figure 2. The optical depth of continental sulfate aerosol is 0.057 at 550-nm wavelength, whereas that of sulfate at urban conditions is 0.57 at the same wavelength.

In the absence of clouds and aerosols, $J(O_3 \rightarrow O(^1D))$ exhibits a weak maximum at about 5-km altitude, which results from the competing effect of a decrease in actinic flux with decreasing altitude and an increase in temperature (the higher the temperature, the higher the O_3 absorption) with decreasing altitude. When $(NH_4)_2SO_4$ aerosol is added to a clear atmosphere, $J(O_3 \rightarrow O(^1D))$ increases everywhere except at the surface, because the increased diffuse actinic flux offsets the loss in direct actinic flux at the surface. As shown by numerous other studies, the presence of a cloud layer (no aerosol) increases J values above and within the upper part of the cloud, while reducing J values below and within the lower portion of the cloud. The addition of $(NH_4)_2SO_4$ aerosol to the cloudy atmosphere mainly increases $J(O_3 \rightarrow O(^1D))$ above and at the top of the cloud layer, but the magnitude of the increase is smaller than that resulting from $(NH_4)_2SO_4$ aerosol under clear sky conditions, because the cloud layer shields the scattering effect of sulfate aerosol located below the cloud layer. $J(NO_2)$ and $J(HCHO)$ exhibit aerosol and cloud effects similar to those for $J(O_3 \rightarrow O(^1D))$.

To examine the effect of solar zenith angle, we consider urban sulfate only, since the effect of sulfate aerosol at continental background levels on J values is small. At a solar zenith angle of 60° (Figure 3), J values are significantly reduced compared with their values at 0° solar zenith angle (Figure 2). There is a crossover of J values for no cloud/no aerosol and no cloud/pure sulfate at an altitude of about 1 km, which is a result of the fact that at larger solar zenith angles the stronger backscattering by sulfate aerosol [*Wiscombe and Grams*, 1976] reduces the available UV flux near the surface but increases it at higher altitudes. Above the cloud layer, urban sulfate aerosol slightly increases J values at higher altitudes (about 4 km here), while it reduces the cloudy sky J values between the top of the cloud layer and 4-km altitude. There are two reasons for this behavior: First, in the scenario considered, about 48% of the total mass of sulfate aerosol is located below the cloud layer. As solar zenith angle increases, the optical path through the cloud increases, producing the same effect as that of a thicker cloud layer. Backscattering by sulfate aerosol below the cloud layer is almost completely shielded, and the small change in J above the cloud layer is produced solely by sulfate aerosol located above the cloud layer. Second, above the cloud layer, sulfate aerosol has the same effect as it does under clear sky conditions; that is, it increases J values above and within the upper part of the aerosol layer but reduces them within the lower part of the aerosol layer.

4.2. Effect of Soot Aerosol on Photolysis Rates

The effect of soot aerosol on $J(O_3 \rightarrow O(^1D))$, $J(NO_2)$, and $J(HCHO)$ at 0° solar zenith angle is shown in Figure 4 for continental soot conditions (optical depth $\tau_{soot} = 0.012$ at a wavelength of 550 nm) and for urban soot conditions ($\tau_{soot} = 0.12$ at the same wavelength). Soot aerosol in the cloud-free atmosphere reduces J values at all altitudes, with the maximum reduction occurring near the surface where the soot mass concentration is highest. In the cloudy atmosphere, soot aerosol absorbs both incident radiation and radiation

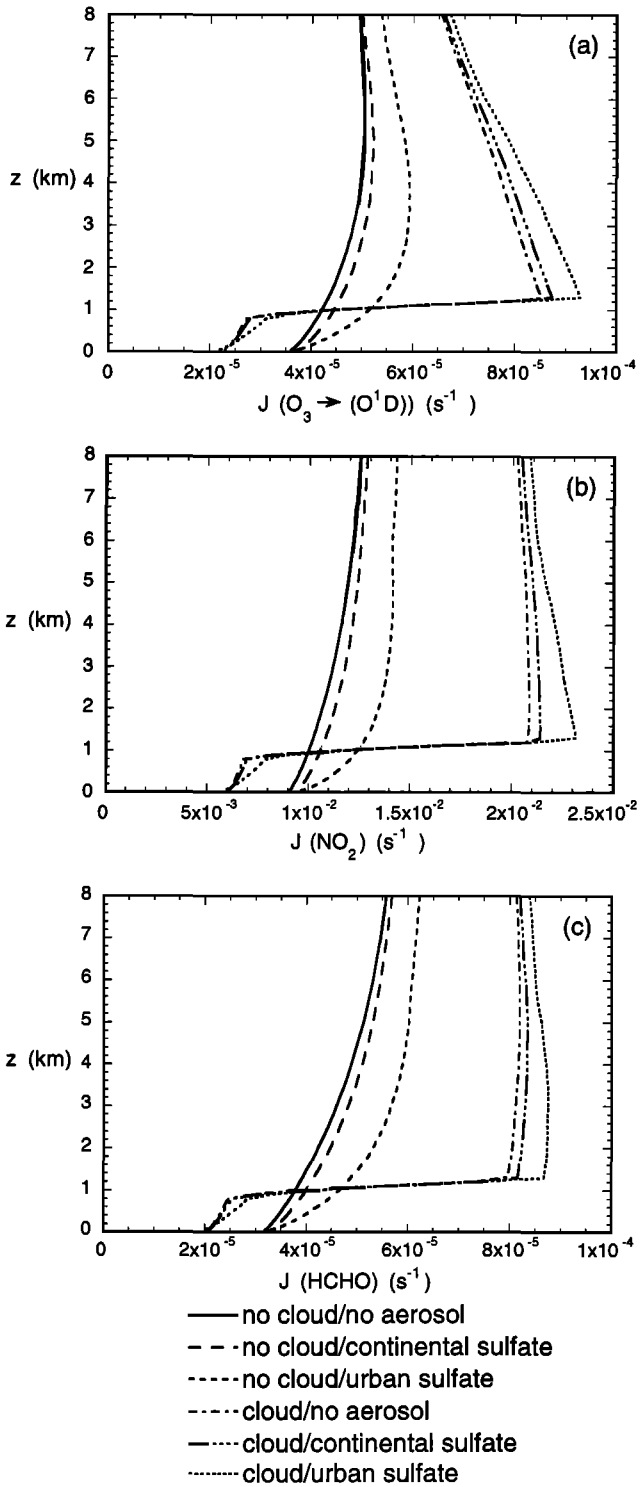

Figure 2. Vertical profiles of (a) $J(O_3 \rightarrow O(^1D))$, (b) $J(NO_2)$, and (c) J(HCHO) at 0° solar zenith angle with and without cloud layer. The effect of sulfate aerosol is presented for both continental and urban conditions. Cloud layer has a thickness of 500 m and is centered at 950-m altitude.

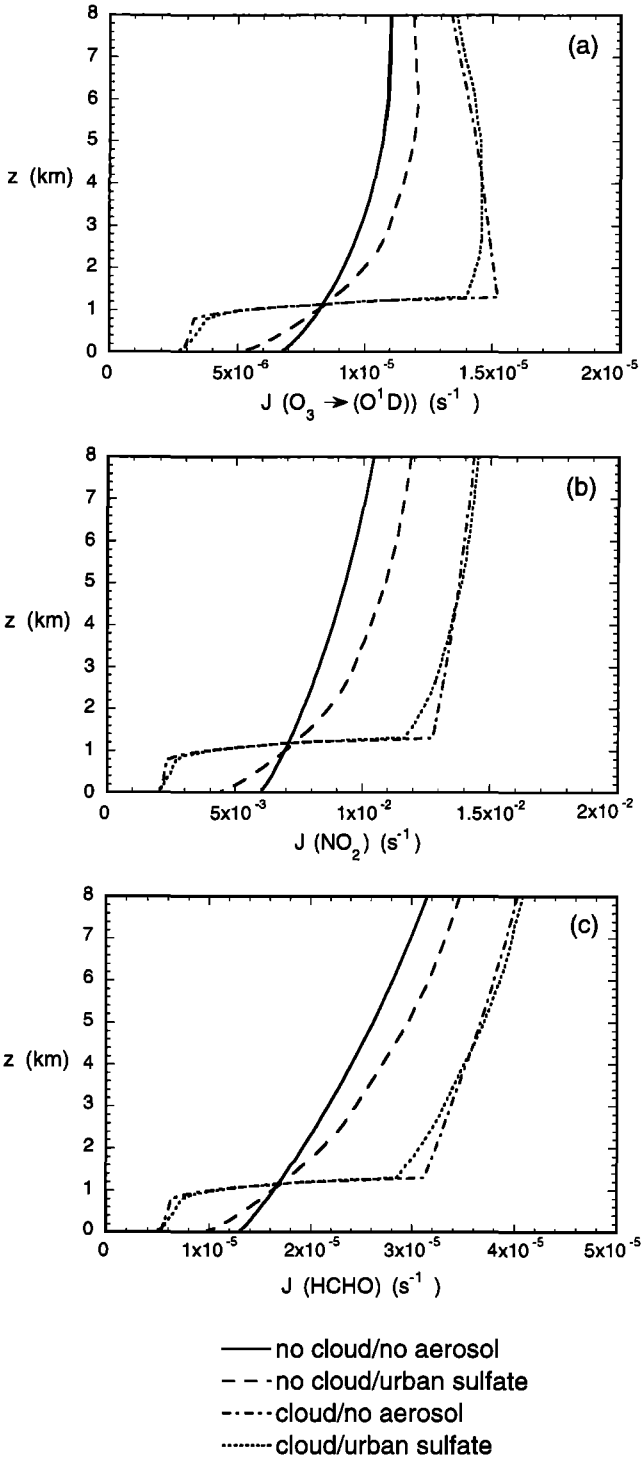

Figure 3. Vertical profiles of (a) $J(O_3 \rightarrow O(^1D))$, (b) $J(NO_2)$, and (c) J(HCHO) at 60° solar zenith angle with and without cloud layer. Pure sulfate is at urban conditions. Cloud layer has a thickness of 500 m and is centered at 950-m altitude. Note the horizontal scale is different from that used in Figure 2.

reflected by the high-albedo cloud layer; hence it significantly reduces J values above the cloud layer, with the magnitude of reduction several times higher than that under clear sky conditions.

Under background continental conditions, soot aerosol has a small effect on clear sky J values but can noticeably reduce photolysis rates when clouds are present; for the conditions considered in Figure 4, continental soot aerosol

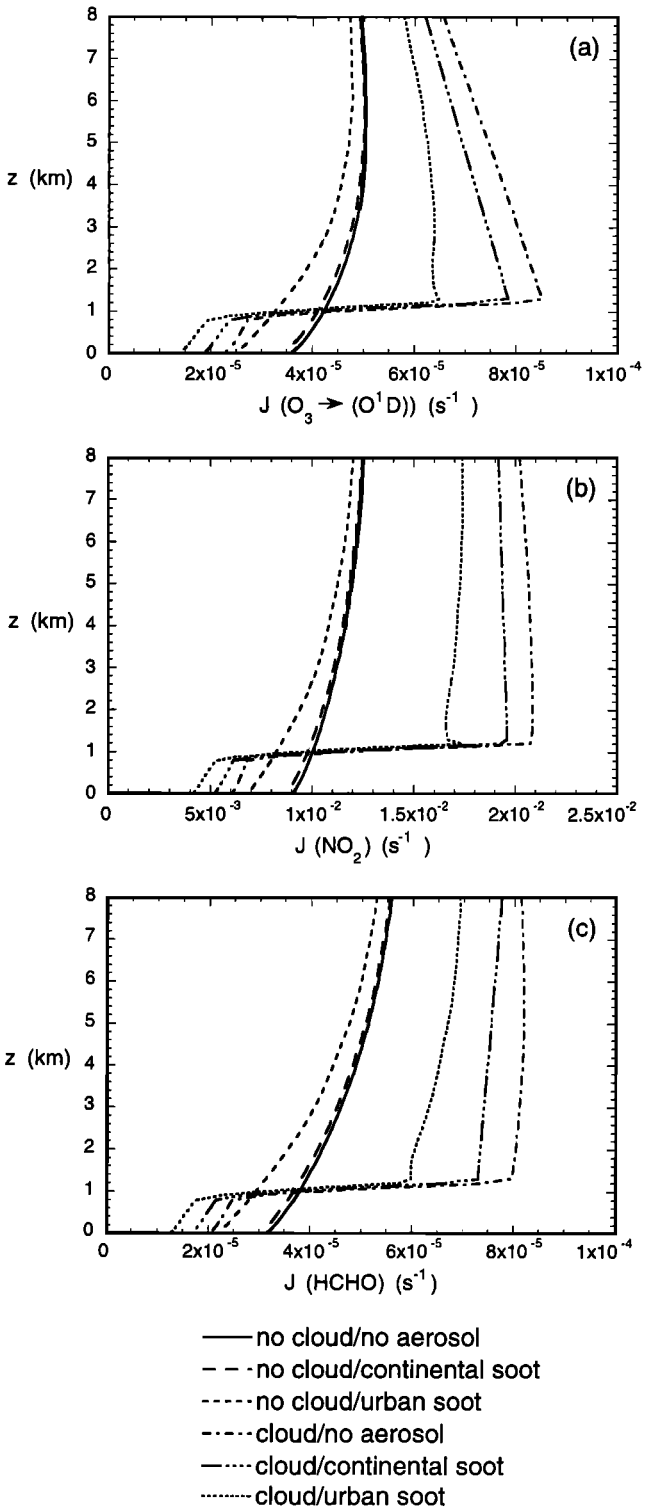

Figure 4. Vertical profiles of (a) $J(O_3 \rightarrow O(^1D))$, (b) $J(NO_2)$, and (c) J(HCHO) at 0° solar zenith angle with and without cloud layer. The effect of soot aerosol is presented for both continental and urban conditions. Cloud layer has a thickness of 500 m and is centered at 950-m altitude.

can reduce J values above the cloud by about 8%. For a solar zenith angle of 60° (not shown), photolysis rates exhibit the same form as those in Figure 4 but shift to smaller values.

4.3. Effect of Internal and External Aerosol Mixtures on Photolysis Rates

Atmospheric aerosols exist as mixtures. For the two species, $(NH_4)_2SO_4$ and soot, in an internal mixture, every particle contains both species, whereas an external mixture consists of pure $(NH_4)_2SO_4$ particles and pure soot particles. With every particle exhibiting some absorption, an internal mixture has a lower single-scattering albedo than the corresponding external mixture does [*Haywood and Shine*, 1995].

$J(O_3 \rightarrow O(^1D))$ in the absence or presence of the 500-m cloud layer is shown in Figure 5 for four cases: (1) no aerosol, (2) pure soot, (3) internal mixture, and (4) external mixture. The internal and external mixtures contain the same amount of soot as that in the pure soot aerosol, but they contain additional sulfate aerosol. Figure 5a is for 0° solar zenith angle, whereas Figure 5b corresponds to 60° solar zenith angle. The behavior of $J(NO_2)$ and J(HCHO) is similar to that of $J(O_3 \rightarrow O(^1D))$ and is not shown here.

Consider first the behavior of $J(O_3 \rightarrow O(^1D))$ at a solar zenith angle of 0°. Under cloud-free conditions, an internal mixture causes a slight reduction in $J(O_3 \rightarrow O(^1D))$ above a certain altitude (2 km for the present conditions), while an external mixture causes an increase in $J(O_3 \rightarrow O(^1D))$ there as a result of the higher single-scattering albedo. Since aerosol concentration is assumed to increase linearly with decreasing altitude, the reduction of $J(O_3 \rightarrow O(^1D))$ by both internal aerosol mixtures and external aerosol mixtures increases rapidly as the altitude decreases. The presence of $(NH_4)_2SO_4$ in the mixtures causes the extinction coefficient of the mixtures to be higher than that of pure soot. Thus the reduction in $J(O_3 \rightarrow O(^1D))$ near the surface in the presence of either an internal mixture or an external mixture is greater than that caused by pure soot. When a cloud is present, both internal mixtures and external mixtures reduce $J(O_3 \rightarrow O(^1D))$ at all altitudes, with the internal mixture always leading to a larger reduction than that of the external mixture. Because the absorption coefficient of an internal mixture is larger than that of pure soot, but since the internal mixture also contains sulfate, its scattering effect is much stronger than that of soot alone. In the presence of a thick cloud, absorption is accentuated; thus absorption by the internal mixture becomes stronger that that by pure soot [*Liao and Seinfeld*, 1998].

At a solar zenith angle of 60°, when no cloud is present, because of the increased upscattering by sulfate at higher solar zenith angles, the mixtures lead to a reduction in $J(O_3 \rightarrow O(^1D))$ below 5-km altitude, producing a crossover of $J(O_3 \rightarrow O(^1D))$ for pure soot and that for mixtures at about 1.5-km altitude. In the presence of the cloud layer, mixtures cause a larger reduction in $J(O_3 \rightarrow O(^1D))$ between the top of the cloud layer and about 4-km altitude than pure soot does.

In summary, aerosol mixtures may either increase or decrease J values under clear sky conditions, depending on the mixture single-scattering albedo, solar zenith angle, and altitude. Regardless of whether aerosol mixtures enhance or reduce J values in a clear atmosphere, they always lead to a reduction in J values in the presence of a cloud.

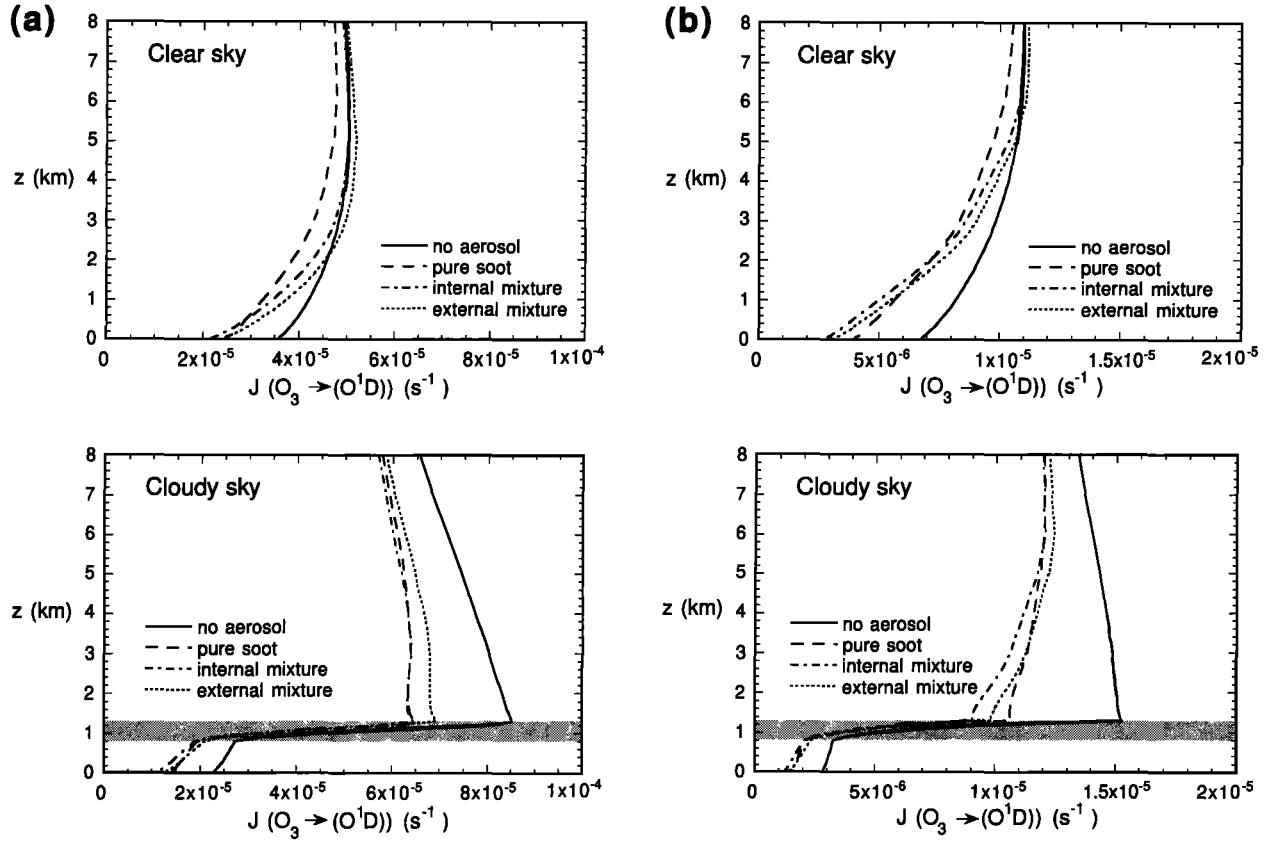

Figure 5. Vertical profiles of $J(O_3 \rightarrow O(^1D))$ for pure soot, internal $(NH_4)_2SO_4$ - soot, and external $(NH_4)_2SO_4$ - soot mixtures with and without cloud layer. Left column (a) is for 0° solar zenith angle and the right column (b) is for 60° solar zenith angle. Shaded region is the cloud layer that has a thickness of 500 m and is centered at 950-m altitude.

4.4. Effect of Mineral Dust Aerosol on Photolysis Rates

Mineral dust aerosol in the lowest several kilometers of the atmosphere exerts the same effect on photolysis rates as that of the sulfate-soot mixtures studied does. The effect of an elevated layer of mineral dust aerosol on $J(O_3 \rightarrow O(^1D))$ is shown in Figures 6a and 6b, where a vertically uniform dust layer of column burden 100 mg m^{-2} is assumed to be located at 3-6 km. In a clear atmosphere, at 0° solar zenith angle, the dust layer reduces photolysis rates at all altitudes, with maximum reduction occurring within the dust layer itself. At 60° solar zenith angle, the upscattering by mineral dust is increased; thus maximum reduction in clear sky J shifts to the bottom of or below the dust layer. In the presence of the cloud layer, an elevated dust layer reduces J above cloud at all solar zenith angles. The effect of an elevated layer of mineral dust on all other J values is similar to that on $J(O_3 \rightarrow O(^1D))$ and thus is not shown here.

5. Effect of Cloud Thickness on Photolysis Rates

To examine the effect of cloud thickness on photolysis rates, we compute $J(O_3 \rightarrow O(^1D))$ (Figure 7) at the two altitudes of 5 km (above cloud and at the top of the aerosol layer) and 300 m (below cloud) as a function of cloud thickness. Urban sulfate and soot are considered here at a solar zenith angle of 0°. The behavior of $J(O_3 \rightarrow O(^1D))$ is representative of that of other photolysis reactions.

At 5 km, the presence of sulfate aerosol always increases J values at any cloud thickness, with the fractional increase becoming smaller as the cloud layer gets thicker. This behavior is expected because of the shielding effect of the cloud. In contrast, soot aerosol always reduces J, with the fractional reduction increasing as cloud thickness increases. The larger the cloud albedo, the greater the amount of radiation reflected back to the soot aerosol above the cloud and absorbed.

At 300-m altitude (below cloud), aerosol effects are maximum under clear sky conditions. As the cloud layer becomes thicker, the sulfate effect quickly becomes negligible, whereas the relative reduction in J by soot aerosol gets somewhat smaller.

6. Uncertainties in Predicted Effects

Uncertainties in the absolute values of the modeled photolysis rates are not a result of the mathematical methods used to solve the radiative transfer equations. The main sources of inaccuracy are incomplete or insufficient input parameters [*Weihs and Webb*, 1997; *Reuder and Schwander*, 1999]. Photolysis rates predicted with models depend on parameters that include solar zenith angle, surface albedo, spectral resolution, vertical resolution, number of radiative

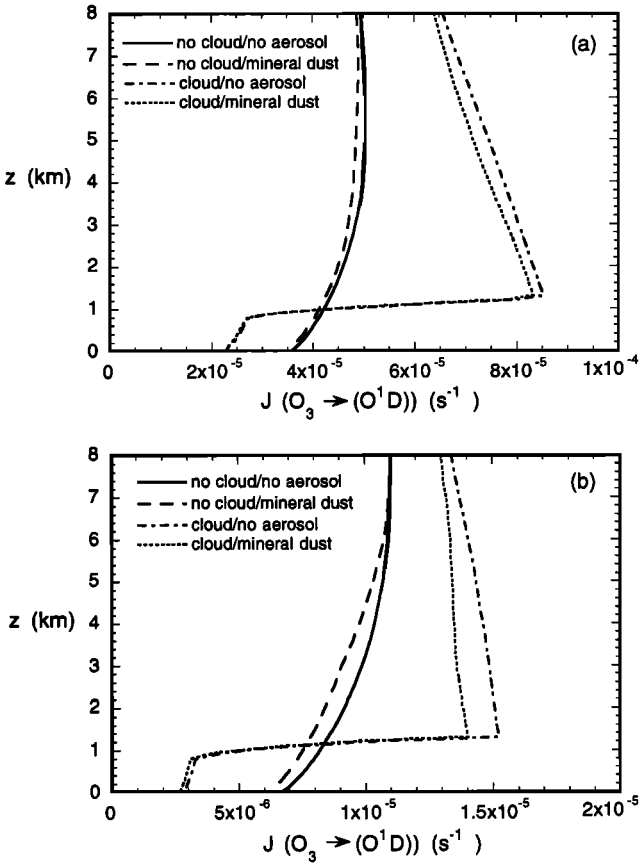

Figure 6. Vertical profiles of $J(O_3 \rightarrow O(^1D))$ in the presence of an elevated layer of mineral dust aerosol with and without cloud layer. (a) solar zenith angle = 0° (b) solar zenith angle = 60°. Dust layer is located at 3-6 km, while the 500-m thick cloud layer is centered at 950-m altitude. Note (a) and (b) have different horizontal scales.

streams, vertical profile of ozone, absorption cross section and quantum yield data for specific species, as well as optical properties (optical depth, single-scattering albedo, and asymmetry factor) of aerosols and clouds. Sensitivity studies have shown that among these parameters, the most important are solar zenith angle, surface albedo, column burden of ozone, and optical properties of aerosols and clouds [*Demerjian et al.*, 1980; *Ruggaber et al.*, 1994]. Since the effects of solar zenith angle, different aerosol types, and cloud thickness have been studied in previous sections, only the effects of surface albedo and ozone column burden will be discussed here.

We have considered urban and continental aerosols in our study because the effect of marine aerosol is expected to be small as a result of its small optical depth. For land surfaces, the albedo depends on the type and amount of vegetation, the type and moisture content of the soil, snow cover, solar zenith angle, and wavelength. One important land surface condition to examine is a surface with fresh snow cover. A wavelength-independent surface albedo of 0.8 is assumed, and we consider both urban sulfate conditions and urban soot conditions at 0° solar zenith angle. Results are compared with those shown in Figures 2 and 4 to investigate the effect of surface albedo when it is changed from the value used by *Demerjian et al.* [1980] to 0.8. Qualitatively, effects of aerosols on photolysis rates at high albedo are the same as those obtained with the previous albedo of Demerjian et al. For the case of urban sulfate, the high albedo leads to a decrease in the effect on photolysis rates with increasing height under clear sky conditions, since multiple scattering is strongest near the surface. For the case of urban soot, the high albedo causes a more significant reduction in both clear sky photolysis rates and cloudy sky photolysis rates; while urban soot aerosol reduces photolysis rates by about 10-20% when the surface albedo is that used by Demerjian et al., it can reduce photolysis rates at all altitudes by about 30-40% over high-albedo surfaces.

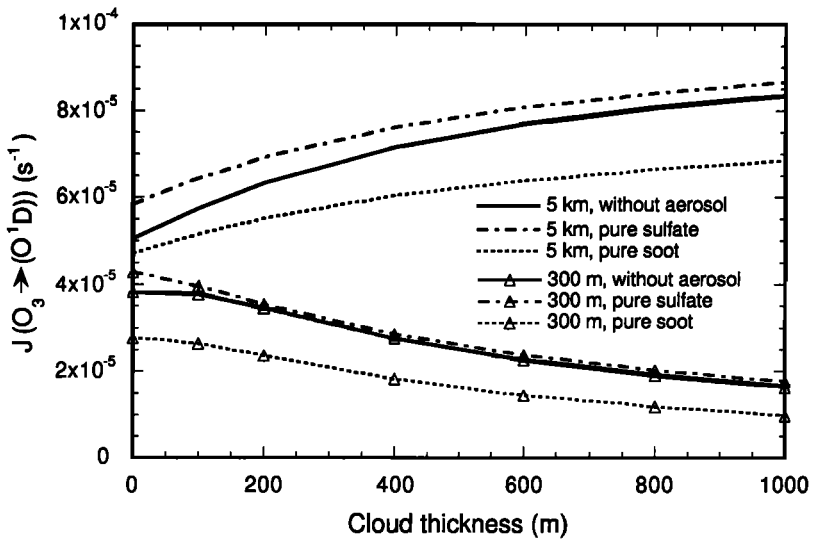

Figure 7. $J(O_3 \rightarrow O(^1D))$ at altitudes of 5 km and 300 m as a function of cloud thickness for three cases: (1) no aerosol; (2) pure sulfate aerosol under urban conditions, and (3) pure soot aerosol under urban conditions. Cloud layer of liquid water content 0.2 g m^{-3} and effective droplet radius 10 μm centered at 950-m altitude.

Table 3. Effects of Urban Sulfate and Soot on Tropospheric Averaged Photolysis Rates

Photolysis Reactions	J_i(no aerosol/no cloud)	J_i (Aerosol/No Cloud)/ J_i (No Aerosol/No Cloud)		J_i (no aerosol/cloud)	J_i (Aerosol/Cloud)/ J_i (No Aerosol/Cloud)	
		sulfate	soot		sulfate	soot
$O_3 \rightarrow O(^3P) + O_2$	4.92×10^{-4}	1.12	0.93	7.74×10^{-4}	1.05	0.89
$O_3 \rightarrow O(^1D) + O_2$	4.78×10^{-5}	1.15	0.91	6.79×10^{-5}	1.05	0.83
$NO_2 \rightarrow NO + O$	1.16×10^{-2}	1.18	0.92	1.91×10^{-2}	1.05	0.83
$NO_3 \rightarrow NO + O_2$	2.79×10^{-2}	1.11	0.94	4.42×10^{-2}	1.04	0.91
$NO_3 \rightarrow NO_2 + O$	2.13×10^{-1}	1.12	0.94	3.42×10^{-1}	1.05	0.90
$N_2O_5 \rightarrow NO_3 + NO_2$	4.46×10^{-5}	1.18	0.89	6.86×10^{-5}	1.06	0.81
$H_2O_2 \rightarrow OH + OH$	9.77×10^{-6}	1.17	0.90	1.50×10^{-5}	1.05	0.81
$HONO \rightarrow OH + NO$	2.69×10^{-3}	1.18	0.92	4.37×10^{-3}	1.05	0.83
$HO_2NO_2 \rightarrow HO_2 + NO_2$	4.68×10^{-6}	1.16	0.91	6.92×10^{-6}	1.05	0.82
$HO_2NO_2 \rightarrow OH + NO_3$	2.30×10^{-6}	1.16	0.91	3.41×10^{-6}	1.05	0.82
$HCHO \rightarrow HCO + H$	4.92×10^{-5}	1.17	0.90	7.50×10^{-5}	1.05	0.81
$HCHO \rightarrow CO + H_2$	7.22×10^{-5}	1.17	0.91	1.14×10^{-4}	1.05	0.81
$CH_3OOH \rightarrow CH_3O + OH$	8.17×10^{-6}	1.17	0.91	1.26×10^{-5}	1.05	0.81
$CH_3COCH_3 \rightarrow$ Products	1.26×10^{-6}	1.14	0.92	1.81×10^{-6}	1.05	0.83

Cloud thickness is 500 m, and solar zenith angle is 0°.

Ozone column burden may vary by more than 200 Dobson units (DU) within a year [*Ruggaber et al.*, 1994]. This change in ozone column burden can significantly affect the photolysis rates of the species that dissociate at wavelengths <325 nm. However, our tests have shown that the change of ozone column burden simply shifts the photolysis rate of a species to a smaller or larger value; the qualitative results concerning the effects of aerosols on photolysis rates obtained in sections 4.1-4.4 do not change with varying ozone column burden.

7. Tropospheric Averaged Photolysis Rates

Tropospheric averaged photolysis rates for all the reactions in Table 2 are presented in Table 3 at a cloud thickness of 500 m and a solar zenith angle of 0°. Under clear sky conditions, sulfate aerosol at the urban level increases all J values by 10-18%, while soot aerosol reduces all J values by 6-11%. When the 500-m cloud layer is present, sulfate aerosol increases all J values by about 5%, and soot aerosol reduces J values by amounts between 9 and 19%. The tropospheric average photolysis ratios show again that a cloud layer reduces the effect of sulfate aerosol but enhances that of soot aerosol.

The current results show that urban aerosols produce a change in photolysis rates of the order of 10-20% when averaged through the troposphere. This value can be larger locally. The aerosol effect is significant when we compare it to the general uncertainty in measuring photolysis rates in a clear or cloudy atmosphere. Although the absolute accuracy of photolysis measurements by a spectroradiometer is estimated to be between ±15 and ±20% depending on the quality of the molecular absorption cross section and quantum yield data, at least three quarters of the uncertainties are of systematic nature caused by the calibration of the detectors [*Shetter and Müller*, 1999]. Thus one can expect that the effect of urban and regional aerosols on photolysis rates should be detectable under both clear sky conditions and cloudy sky conditions and that the effect of absorbing aerosols (in the form of internal or external mixtures) at continental conditions should be detectable in the presence of low-level stratus clouds.

8. Conclusions

A one-dimensional radiative model is applied to study the effects of aerosols on tropospheric photolysis rates under both clear sky conditions and cloudy sky conditions. Aerosol types considered are pure sulfate, pure soot, and the mixtures of sulfate and soot, as well as mineral dust. In the absence of clouds, soot aerosol reduces photolysis rates at all altitudes, whereas sulfate aerosol generally increases photolysis rates above and in the upper part of the aerosol layer but reduces photolysis rates in the lower part of the aerosol layer and at the surface. Aerosol mixtures may reduce or increase photolysis rates from those under clear sky conditions, depending on the single-scattering albedo, solar zenith angle, and altitude. An elevated layer of mineral dust aerosol mainly reduces photolysis rates but may increase J values above the layer at high solar zenith angles. The results obtained here for clear sky conditions are consistent with those presented by *Dickerson et al.* [1997] and *Jacobson* [1998].

When a low-level stratus cloud is present, sulfate aerosol may increase photolysis rates above the cloud, but the magnitude of increase is smaller than that resulting from sulfate aerosol under clear sky conditions. Soot aerosol, aerosol mixtures, and mineral dust absorb more radiation and hence reduce photolysis rates above the cloud layer. Even though aerosol mixtures and mineral dust may increase photolysis rates under clear sky conditions, they always lead to a reduction in J values in the presence of low-level clouds.

Acknowledgments. This work was supported by National Science Foundation grant ATM-9614105 and NASA grant NAG5-3553.

References

Castro, T., L. G. Ruizsuarez, J. C. Ruizsuarez, M. J. Molina, and M. Montero, Sensitivity analysis of a UV-radiation transfer model and experimental photolysis rates of NO_2 in the atmosphere of Mexico City, *Atmos. Environ., 31*, 609-620, 1997.

Chandrasekhar, S., *Radiative Transfer*, Dover, Mineola, N.Y., 1960.

Crawford, J., D. Davis, G. Chen, R. Shetter, M. Müller, J. Barrick, and J. Olson, An assessment of cloud effects on photolysis rate coefficients: Comparison of experimental and theoretical values, *J. Geophys. Res., 104*, 5725-5734, 1999.

d'Almeida, G. A., P. Koepke, and E. P. Shettle, *Atmospheric Aerosols: Global Climatology and Radiative Characteristics*, 261 pp, A. Deepak, Hampton, Va., 1991.

Demerjian, K. L., K. L. Schere, and J. T. Peterson, Theoretical estimates of actinic (spherially integrated) flux and photolytic rate constants of atmospheric species in the lower troposphere, *Adv Environ. Sci. Technol.*, *10*, 369-459, 1980.

DeMore, W. B., C. J. Howard, S. P. Sander, A. R. Ravishankara, D. M. Golden, C. E. Kolb, R. F. Hampson, M. J. Molina, and M. J. Kurylo, Chemical kinetics and photochemical data for use in stratospheric modeling, *JPL Publ., 97-4*, 1997.

Dentener, F. J., G. R. Carmichael, Y. Zhang, J. Lelieveld, and P. J. Crutzen, Role of mineral aerosol as a reactive surface in the global troposphere, *J. Geophys. Res., 101*, 22,869-22,899, 1996.

Dickerson, R. R., S. Kondragunta, G. Stenchikov, K. L. Civerolo, B. G. Doddridge, and B. N. Holben, The impact of aerosols on solar ultraviolet-radiation and photochemical smog, *Science*, *215*, 827-830, 1997.

Erlick, C., and J. E. Frederick, Effects of aerosols on the wavelength dependence of atmospheric transmission in the ultraviolet and visible, 2, Continental and urban aerosols in clear skies, *J. Geophys. Res., 103*, 23,275-23,285, 1998.

Erlick, C., J. E. Frederick, V. K. Saxena, and B. N. Wenny, Atmospheric transmission in the ultraviolet and visible: Aerosols in cloudy atmospheres, *J. Geophys. Res., 103*, 31,541-31,556, 1998

Forster, P. M. D., Modeling ultraviolet radiation at the Earth's surface, I, The sensitivity of ultraviolet radiances to atmospheric changes, *J. Appl. Meteorol., 34*, 2412-2425, 1995.

Fuglestvedt, J. S., J. E. Jonson, and I. S. A. Isaksen, Effects of reductions in stratospheric ozone on tropospheric chemistry through changes in photolysis rates, *Tellus, Ser. B,46*, 172-192, 1994.

Gierczak, T., J. B. Burkholder, S. Bauerle, and A. R. Ravishankara, Photochemistry of acetone under tropospheric conditions, *Chem. Phys., 231*, 229-244, 1998.

Hale, G. M , and M R. Querry, Optical constants of water in the 200 nm to 200 mm wavelength region, *Appl. Opt., 12*, 555-563, 1973.

Haywood, J. M., and K. P. Shine, The effect of anthropogenic sulfate and soot on the clear sky planetary radiation budget, *Geophys. Res. Lett , 22*, 603-606, 1995.

Jacobson, M. Z., Studying the effects of aerosols on vertical photolysis rate coefficient and temperature profiles over an urban airshed, *J. Geophys Res., 103*, 10,593-10,604, 1998.

Jacobson, M. Z., Isolating nitrated and aromatic aerosols and nitrated aromatic gases as sources of ultraviolet light absorption, *J. Geophys. Res., 104*, 3527-3542, 1999.

Johnston, H. S., H. F. Davis, and Y. T. Lee, NO_3 photolysis product channels: Quantum yields from observed energy thresholds, *J. Phys. Chem., 100*, 4713-4723, 1996.

Kim, Y. P., J. H. Seinfeld, and P. Saxena, Atmospheric gas aerosol equilibrium, 1, Thermodynamic model, *Aerosol Sci Technol , 19*, 157-181, 1993a.

Kim, Y. P., J H. Seinfeld, and P. Saxena, Atmospheric gas-aerosol equilibrium, 2, Analysis of common approximations and activity-coefficient calculation methods, *Aerosol Sci. Technol., 19*, 182-198, 1993b.

Krol, M. C., and M. van Weele, Implications of variations in photodissociation rates for global tropospheric chemistry, *Atmos. Environ., 31*, 1257-1273, 1997.

Landgraf, J., and P. J. Crutzen, An efficient method for online calculations of photolysis and heating rates, *J. Atmos. Sci., 55*, 863-878, 1998.

Lantz, K. O., R. E Shetter, C. A. Cantrell, S. J. Flocke, J. G. Calvert, and S. Madronich, Theoretical, actinometric, and radiometric determinations of the photolysis rate coefficient of NO_2 during the Mauna Loa Observatory Photochemistry Experiment 2, *J. Geophys. Res., 101*, 14,613-14,629, 1996.

Liao, H., and J. H. Seinfeld, Effect of clouds on direct aerosol radiative forcing of climate, *J. Geophys. Res., 103*, 3781-3788, 1998.

Liu, S. C., and M. Trainer, Responses of the tropospheric ozone and odd hydrogen radicals to column ozone change, *J. Atmos. Chem., 6*, 221-233, 1988.

Liu, S. C., S. A. McKeen, and S Madronich, Effect of anthropogenic aerosols on biologically active ultraviolet radiation, *Geophys. Res. Lett., 18*, 2265-2268, 1991.

Ma, J., Effects of stratospheric ozone depletion on tropospheric chemistry through changes in UV-B radiation, *TNO-MW-R-95/127*, Neth. Organ for Appl. Sci , Delft, Netherlands, 1995

Ma, J., and R. Guicherit, Effects of stratospheric ozone depletion and tropospheric pollution on UV-B radiation in the troposphere, *Photochem. Photobiol., 66*, 346-355, 1997.

Madronich, S., Intercomparison of NO_2 photodissociation and UV radiometer measurements, *Atmos. Environ., 21*, 569-578, 1987a.

Madronich, S., Photodissociation in the atmosphere, 1, Actinic flux and the effects of ground reflections and clouds, *J. Geophys. Res., 92*, 9740-9752, 1987b.

Madronich, S., and C. Granier, Impact of recent total ozone changes on tropospheric ozone photodissociation, hydroxyl radicals, and methane trends, *Geophys. Res. Lett., 19*, 465-467, 1992.

Malicet, J., D. Daumont, J. Charbonnier, C. Parisse, A. Chakir, and J. Brion, Ozone UV spectroscopy, 2, Absorption cross-sections and temperature-dependence, *J. Atmos. Chem., 21*, 263-273, 1995.

Matthijsen, J., P. J. H. Builtjes, E. W. Meijer, and G. Boersen, Modeling cloud effects on ozone on a regional scale: A case study, *Atmos. Environ., 31*, 3225-3236, 1997

Matthijsen, J., K. Suhre, R. Rosset, F. L. Eisele, R. L. Mauldin III, and D. J. Tanner, Photodissociation and UV-radiative transfer in a cloudy atmosphere: Modeling and measurements, *J. Geophys. Res., 103*, 16,665-16,676,1998.

Neckel, H., and D. Labs, The solar radiation between 3300 Å and 12500 Å, *Sol Phys., 90*, 205-258, 1984.

Papayannis, A., D. Balis, A. Bais, H. van der Bergh, B. Calpini, E. Durieux, L. Fiorani, L. Jaquet, I. Ziomas, and C. S. Zerefos, Role of urban and suburban aerosols on solar UV radiation over Athens, Greece, *Atmos. Environ., 32*, 2193-2201, 1998.

Patterson, E. M., D. A. Gillette, and B. H. Stockton, Complex index of refraction between 300 and 700 nm for Saharan aerosols, *J. Geophys. Res., 82*, 3151-3160, 1977.

Pilinis, C , and J. H. Seinfeld, Continued development of a general equilibrium model for inorganic multicomponent atmospheric aerosols, *Atmos. Environ., 21*, 2453-2466, 1987.

Repapis, C. C., H. T. Mantis, A. G. Paliatsos, C. M. Philandras, A. F. Bais, and C. Meleti, Case study of UV-B modification during episodes of urban air pollution, *Atmos. Environ., 32*, 2203-2208, 1998.

Reuder J , and H. Schwander, Aerosol effects on UV radiation in nonurban regions, *J Geophys. Res., 104*, 4065-4077, 1999.

Reuder, J., T. Gori, L. Kins, and R. Dlugi, Determination of photolysis frequencies of ozone and nitrogen dioxide during SANA 2: The influence of tropospheric aerosol particles, *Meteorol. Z. N. F., 5*, 234-244, 1996.

Ruggaber, A., R. Dlugi, and T. Nakajima, Modeling radiation quantities and photolysis frequencies in the troposphere, *J. Atmos. Chem., 18*, 171-120, 1994.

Sander, S P., Temperature-dependence of the NO_3 absorption spectrum, *J. Phys Chem., 90*, 4135-4142, 1986.

Shetter, R. E., and M. Müller, Photolysis frequency measurements using actinic flux spectroradiometry during the PEM-Topics mission: Instrument description and some results, *J. Geophys. Res., 104*, 5647-5661, 1999.

Slingo, A., and H. M. Schrecker, On the shortwave radiative properties of stratiform water clouds, *Q. J. R. Meteorol. Soc., 108*, 407-426, 1982.

Sloane, C. S., Optical properties of aerosols of mixed composition, *Atmos. Environ , 18*, 871-878, 1984.

Sloane, C. S., Effect of composition on aerosol light-scattering efficiencies, *Atmos. Environ., 20*, 1025-1037, 1986.

Sloane, C. S , and G. T. Wolff, Prediction of ambient light scattering using a physical model responsive to relative humidity: Validation with measurements from Detroit, *Atmos Environ., 19*, 669-680, 1985

Sloane, C. S., J. Watson, J. Chow, L. Pritchett, and L. W. Richards, Size-segregated fine particle measurements by chemical species and their impact on visibility impairment in Denver, *Atmos. Environ., Part A, 25*, 1013-1024, 1991

Sokolik, I., A. Andronova, and T. C. Johnson, Complex refractive index of atmospheric dust aerosols, *Atmos. Environ., 27*, 2495-2502, 1993.

Stamnes, K., S. C. Tsay, W. Wiscombe, and K. Jayaweera, Numerically stable algorithm for discrete-ordinate-method radiative transfer in multiple scattering and emitting layered media, *Appl. Opt., 27*, 2502-2509, 1988.

Takahashi, K., N. Taniguchi, Y. Matsumi, M. Kawasaki, and M. N. R. Ashfold, Wavelength and temperature dependence of the absolute $O(^1D)$ production yield from the 305-329 nm photodissociation of ozone, *J. Chem. Phys., 108*, 7161-7172, 1998.

Thompson, A. M., The effect of clouds on photolysis rates and ozone formation in the unpolluted troposphere, *J. Geophys Res*, *89*, 1341-1349, 1984.

Thompson, A. M., M. A. Owens, and R. W. Stewart, Sensitivity of tropospheric oxidants to global chemical and climate change, *Atmos. Environ.*, *23*, 516-532, 1989.

Toon, O. B., J. B. Pollack, and B. N. Khare, The optical constants of several atmospheric aerosol species: Ammonium sulfate, aluminum oxide, and sodium chloride, *J. Geophys. Res.*, *81*, 5733-5748, 1976

Tsay, S. C., and K. Stamnes, Ultraviolet radiation in the arctic: The impact of potential ozone depletions and cloud effects, *J. Geophys Res.*, *97*, 7829-7840, 1992.

van Weele, M., and P. G. Duynkerke, Effect of clouds on the photodissociation of NO_2: Observations and modeling, *J. Atmos Chem.*, *16*, 231-255, 1993.

Weihs, P., and A. R. Webb, Accuracy of spectral UV model calculations, 1, Consideration of uncertainties in input parameters, *J. Geophys. Res.*, *102*, 1541-1550, 1997.

Wiscombe, W. J., The delta-M method: Rapid yet accurate radiative flux calculations for strongly asymmetric phase functions, *J. Atmos. Sci.*, *34*, 1408-1422, 1977.

Wiscombe, W, and G. Grams, The backscattered fraction in two-stream approximations, *J. Atmos. Sci.*, *33*, 2440-2451, 1976

Woods, T. N., et al., Validation of the UARS solar ultraviolet irradiances: Comparison with the ATLAS 1 and 2 measurements, *J. Geophys. Res.*, *101*, 9541-9569, 1996.

World Climate Program, A preliminary cloudless standard atmosphere for radiation computation, report, World Meteorol. Organ., Geneva, 1986.

World Meteorological Organization (WMO), Atmospheric ozone: 1985, Report No. 16, Geneva, 1985.

H. Liao and J. H. Seinfeld, Division of Engineering and Applied Science, California Institute of Technology, Mail Code 104-44, Pasadena, CA 91125. (seinfeld@cco caltech.edu)

Y. L. Yung, Division of Geological and Planetary Sciences, California Institute of Technology, Pasadena, CA 91125.

(Received January 19, 1999; revised June 5, 1999;
accepted June 8, 1999.)